Industrial Crops & Products 184 (2022) 114996

Contents lists available at ScienceDirect

Industrial Crops & Products

journal homepage: www.elsevier.com/locate/indcrop

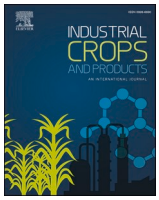

High-performance polylactic acid compressed strawboard using pre-treated and functionalised wheat straw

Mehdi Chougan [a], Seyed Hamidreza Ghaffar [a,*], Ewa Mijowska [b], Wojciech Kukułka [b], Pawel Sikora [c,d]

[a] Department of Civil and Environmental Engineering, Brunel University London, Uxbridge UB8 3PH, United Kingdom
[b] Department of Nanomaterials Physicochemistry, Faculty of Chemical Technology and Engineering, West Pomeranian University of Technology, Al. Piastow 45, 70-311 Szczecin, Poland
[c] Faculty of Civil and Environmental Engineering, West Pomeranian University of Technology in Szczecin, Al. Piastow 50, 70-311 Szczecin, Poland
[d] Building Materials and Construction Chemistry, Technische Universität Berlin, Gustav-Meyer-Allee 25, 13355 Berlin, Germany

ARTICLE INFO

Keywords:
Polylactic acid compressed strawboards
Wheat straw
Attapulgite nanoclay
Graphene nanoplatelets
Pre-treatment
Surface functionalization

ABSTRACT

An eco-friendly pre-treatment coupled with surface functionalisation were developed to enhance the quality of wheat straw particles to be used for development of high-performance polylactic acid (PLA) compressed strawboard. Eco-friendly hybrid pre-treatment (i.e., hot water followed by steam, H+S) and surface functionalisation processes employing attapulgite nanoclay (AT) and graphene nanoplatelets (G) were used to obtain an appropriate wheat straw surface quality while increasing its compatibility with the PLA matrix. The successful pre-treatment and surface functionalisation of wheat straw particles was verified through characterisation techniques, including SEM, FTIR, XRD, Raman spectroscopy, and TGA. Tensile strength and water absorption properties of compressed strawboards were examined to investigate the influence of pre-treatment and surface functionalisation of wheat straws. The maximum tensile strengths of 28 MPa and 27 MPa were recorded for 10 H+S-AT and 10 H+S-G samples, respectively, which are considerably higher than the value (i.e., 9.7 MPa) registered for the sample without pre-treatment and surface functionalisation (i.e., 10UN). The lowest water absorption after 24 h of immersion was registered for 10UN-G (i.e., 1.6%), which is 11% and 31% lower than the 10UN and 10 H+S samples, respectively. The effect is attributed to an improved interfacial bond between wheat straw and PLA matrix due to the graphene surface functionalisation, as evidenced by the SEM.

1. Introduction

Polylactic acid (PLA) is among the most prominent biodegradable polymers and has considerable ability of replacing petroleum-based plastics. PLA is made from fermented lactic acid derived from renewable agricultural sources such as corn and wheat. PLA has a broader range of applications than other biodegradable polymers due to its superior mechanical characteristics, biocompatibility and biodegradability, ease of processing, and thermal stability (Gupta et al., 2007; Tawakkal et al., 2014). However, PLA is far more expensive than its petroleum-based competitors, severely limiting its commercial application in the industrial sector (Qin et al., 2011). Recent research suggests replacing the PLA matrix with low-cost agricultural waste components to alleviate this problem. Various types of agricultural waste materials, including hemp and jute strands, corn cobs, and rice husks have received a lot of research attention as a possible eco-friendly replacements in bio-based composites (Liu et al., 2017; Melo et al., 2014; Tribot et al., 2018). Wheat straw, a renewable agricultural biomass with chemical constituents of cellulose, hemicellulose, lignin, and extractives, has the potential to successfully substitute polymer matrix in a variety of applications. Nevertheless, its high concentration of hydrophobic elements, i.e., waxy cuticle layers, inorganic silica, and extractives, results in inadequate surface characteristics, impairing the interfacial bond quality between the wheat straw and polymer binder (Ghaffar et al., 2017a; Ghaffar and Fan, 2017, 2015).

Pre-treatment and coating processes have been introduced as a feasible approach to overcome these shortcomings in numerous efforts (Ghaffar et al., 2017b; Ghaffar and Fan, 2015; Hýsková et al., 2020). To improve adhesion between biomass and polymer matrix and, as a result, the ultimate performance of bio-based composites, a variety of

* Corresponding author.
E-mail address: seyed.ghaffar@brunel.ac.uk (S.H. Ghaffar).

https://doi.org/10.1016/j.indcrop.2022.114996
Received 26 November 2021; Received in revised form 2 April 2022; Accepted 24 April 2022
Available online 18 May 2022

pre-treatment solutions have been developed, which can be classified into physical and chemical methods. When evaluating sustainability, it should be highlighted that although chemical pre-treatments substantially modify biomass structure, they may not be economically feasible, and the required chemicals could be hazardous. Thus their environmental implications would be unfavourable compared to that of physical pre-treatments (Chougan et al., 2020; Fan et al., 2018). For instance, pre-treatment techniques such as alkaline chemical, microwave, boiling and steaming, and enzymatic pre-treatments were used to enhance the performance of bio-based PLA composites (Laadila et al., 2017). In addition, coupling agents such as silane coupling agent were used to improve the compatibility interface and thermal stability performance of wheat straw/PLA composites (Chen et al., 2021).

Depending on the size and origin of the filler biomass resources, bio-based PLA composites have been used in various applications. Composites using micron-sized biomass materials could be a valuable source for developing single-use plastics, cutlery, and food packaging. To eliminate the use of chemicals in food-grade applications, Mousa et al. (2022) used biomass filler derived from date palm rachis without any chemical treatments or surface modification (Mousa et al., 2022). In addition, reduced density, fire resistance, acoustic emission resistance, low cost, availability, high energy efficiency, and an appropriate modulus-weight ratio makes it suitable for non-load bearing applications in the construction and automotive industries (Das et al., 2022; Pawar et al., 2022; Prakash et al., 2022).

This study utilised a selective separation of wheat straw nodes that serve as defects in bio-based composites to optimize the bonding efficiency between wheat straw particles and polymer matrix. Thereupon, a light physical pre-treatment (H+S) was employed to improve the surface properties of wheat straw particles. This pre-treatment method was chosen based on the author's previous study in which H+S demonstrated a positive effect on the extraction of undesirable chemicals and improvements in tensile strength (Chougan et al., 2020). Graphene nanoparticles and attapulgite nanoclay at 0.1 wt.-% and 1 wt.-% weight percent, respectively, were used to functionalise the surfaces of both untreated and pre-treated straws. The author's previous study investigated the same surface functionalisation system, which confirms the nanomaterial's surface modification role in improving the interfacial bonding between cementitious composite matrix and straw particles (Chougan et al., 2022). To the best of the authors' knowledge, no studies on wheat straw has implemented the pre-treatment coupled with surface functionalisation with graphene and attapulgite nanoparticles to be employed in bio-based polymer composites. Extensive material characterisations, including FTIR, SEM, Raman, XRD, and TGA, were carried out to confirm the adequate surface functionalisation of wheat straw particles. Bulk property evaluation of PLA compressed strawboard was also performed in order to assess the impacts of surface functionalisation and pre-treatment processes on potential enhancements of mechanical

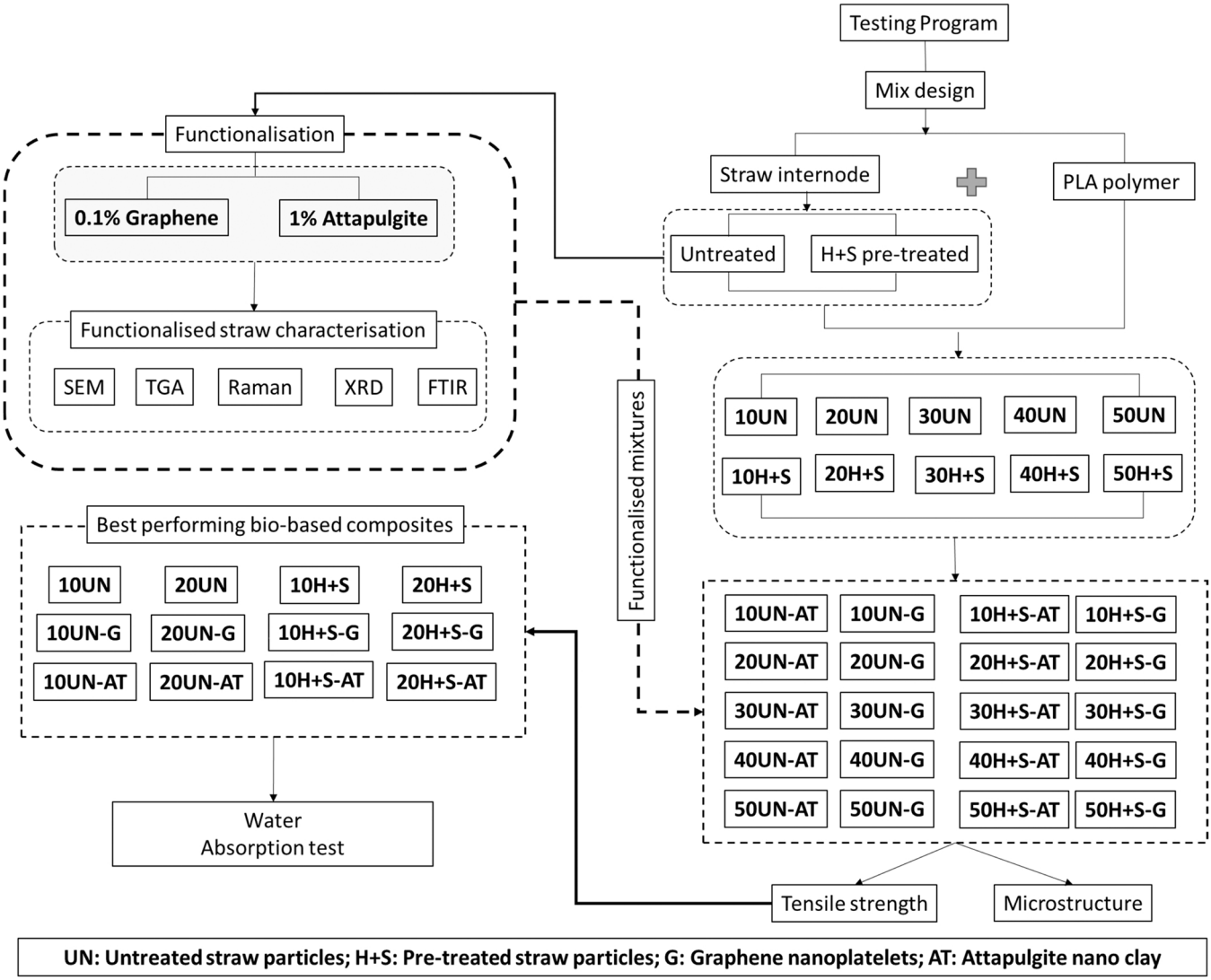

Fig. 1. Schematic structure of experimental testing programme.

performance and dimensional stability.

The testing procedure and investigation strategy for this research is depicted in Fig. 1.

2. Materials and method

Thermoplastic polylactic acid (PLA) used as matrix in this work was purchased from Tecnaro GmbH's Ilsfeld, Germany. Wheat straw biomass (*Triticum aestivum* L.) was supplied from a residential farm (Middlesex, UK) harvested in late summer 2019. Two different coupling agent nanomaterials, were employed for surface functionalisation, namely, attapulgite nanoclay (AT) supplied by Lawrence Industries Ltd., UK, and graphene nanoplatelets (G), provided by Nanesa S.r.l., Italy. Microstructure images of G, AT are presented in Fig. 2 (a and b). A fringed shape with a wrinkling surface was highlighted for isolated graphene nanoplatelets. These particles accumulate into large agglomerates, as seen by the distinctive shape of specimens produced from expanded graphite flakes. AT particles, however, exhibit a rough surface and an angular morphology with sharp edges. The detailed characterization of both G and AT particles was presented in the author's previous studies (Chougan et al., 2021; Lamastra et al., 2021). Based on the supplier's information (i.e., Nanesa S.r.l. for graphene, and Lawrence Industries Ltd. for attapulgite), the industrial-scale cost of functionalising agents is approximately 70 €/kg and 6 €/kg for graphene and attapulgite, respectively. Consequently, the estimated production cost of strawboard of size 1 m^3 with 20 vol% straw replacement will be increased around € 5.5 and €4.5 by the incorporation of 0.1% graphene and 1% attapulgite particles. It should be noticed that due to scientific research in our study the attapulgite clay was obtained from chemical company therefore its price was high. However, there are many nanoclay deposits available globally as this is naturally occurring material, thus it's price could decreased when the material is commercialised.

2.1. Wheat straw preparation, pre-treatment, and functionalisation

Prior to the pre-treatment and surface functionalization processes, as-received wheat straw was cleaned and oven-dried at 100 ± 5 °C for 24 h (Fig. 3-i). Based on the author's previous work (Ghaffar and Fan, 2015), due to inconsistent shape and chemical functional groups distribution throughout the straw stem, only the internode was used for bio-based composites. Straw internode sections were shredded to obtain straw particles using a Retsch SM 100 cutting mill. More than 99% of the straw particles were found to be in the range of 65 – 2000 μm (see Fig. 2 c).

An eco-friendly and hazardous-substance-free pre-treatment combining hot water (H) and steaming (S) was carried out on wheat straw particles (Fig. 3-ii). Throughout the (H) stage, straw particles were introduced into a pressure cooker for 60 min at a constant pressure of approximately 0.1 MPa. Then, boiled-straw particles were steamed immediately for another 30 min using a mesh basket positioned directly above boiling water. Both pre-treated (H+S) and untreated (UN) straw particles were used in order to investigate the effect of surface functionalisation. Before surface functionalisation stage, to achieve an effective dispersion of attapulgite nanoclay (AT) and graphene nanoplatelets (G), an ultra-sonication technique in an aqueous solution was performed. The ultrasonic time and power were set to 90 min and 200 W/cm^2, respectively. In this study, the optimum concentrations of 0.1 wt% and 1 wt% were utilised for AT and G, respectively, which have been reported in previous investigations (Scaffaro et al., 2020; Zhu et al., 2019). Correspondingly, (UN) and (H+S) straw particles were introduced in pre-dispersed G and AT aqueous solutions. The straw particles and pre-dispersed solution were stirred for 12 h at 80 °C using a hot plate and magnetic stirrer until 90% water was evaporated from the solution (Fig. 3-iii). Each sample was then oven-dried at 100 °C for 24 h, where the AT and G particles stick to the outer surface of UN and H+S straw particles. More details on surface functionalisation and pre-treatment procedures can be found in the author's previous research papers (Chougan et al., 2022, 2020). The authors believe that the proposed pre-treatment (i.e., H+S) could limit energy use as well as involvement of chemical agents in comparison to bleaching, alkaline oxidation, and plasma. It is acknowledged that the wastewater generated by the H+S pre-treatment could contain hazardous substances, however compared to the chemical pre-treatments and disposal of agricultural waste materials in the environment (e.g., burning), the H+S is relatively considered as eco-friendly. Moreover, as per author's previous study, it is evident that the extractives in nodes are 10–15% higher than in internodes. Therefore, removing node section before pre-treatment guarantees the minimum release of these substances in the environment (Ghaffar and Fan, 2017). It is worth noting that based on the author's experience, all the wastewater in the boiling stage of the pre-treatment will evaporate during the steaming stage.

2.2. Compressed strawboard sample preparation

A total of 30 compressed strawboards were fabricated using H+S and UN straw particles and their surface functionalised derivatives, i.e., UN-G, UN-AT, H+S-G, and H+S-AT. PLA polymer pellets were replaced by wheat straw particles with volume ratios of 10, 20, 30, 40, and 50 (see Table 1). For each composition, straw particles were dry-mixed with polymer pellets to ensure the uniform distribution of materials. The mixture was placed into the steel mould of 100 mm × 100 mm x 20 mm and heated in the hot-air oven for 15 min at 180 ± 10 °C to facilitate the PLA melting process. After the pre-heating step, straw particles were mixed with polymer pellets to ensure uniform distribution, the mould with softened PLA and straws was then hot-pressed (see Fig. 3-iiii) for 20 min at 180 °C under the pressure of 10 MPa. Samples were subjected

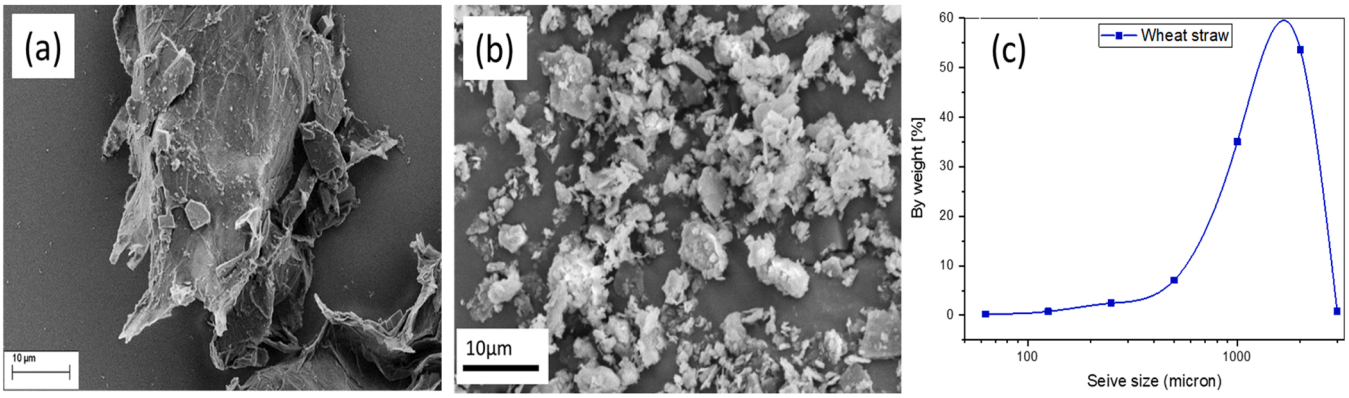

Fig. 2. Microstructure profile of (a) graphene nanoplatelets, (b) attapulgite nanoclay and (c) particle size distribution analysis of wheat straw particles.

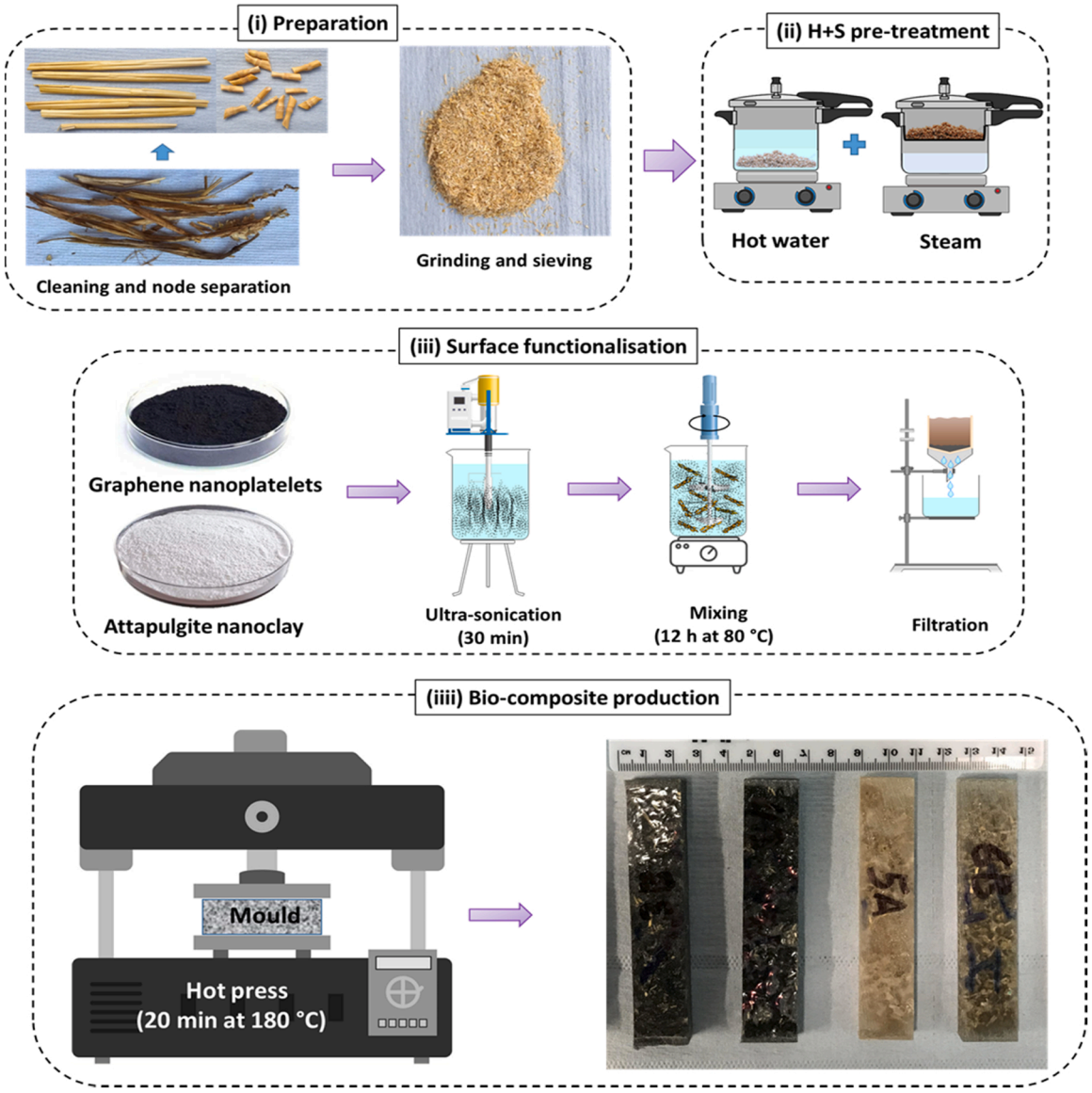

Fig. 3. Schematic framework of different stages of wheat straw board preparation.

to a 15 kg weight immediately after removing the moulds from the hot-press to prevent the samples from expanding. Subsequently, the resulting bio-composite was allowed to cool down for 20 min to reach room temperature. Finally, specimens for the tensile test were taken by cutting the bio-composites into 20 mm wide strips.

2.3. Characterisations and testing of functionalised wheat straw

2.3.1. Microstructure

Scanning electron microscopy (SEM, VEGA3 TESCAN) was used to examine the surface morphology and microstructure of functionalised wheat straw samples and compare them to control specimens. Ten straw particles with a size of 5 mm^3 were examined for each composition to observe the surface alterations induced as a result of surface functionalisation. A total of ten specimens with an approximate size of 10 mm^3 were taken from fractured sections of composite samples in tensile testing to analyse the interfacial bonding between the functionalised straw particles and polymer matrix. Samples were chromium-coated to ensure appropriate electrical conductivity.

2.3.2. Raman spectroscopy

In order to characterise the presence of functionalising agents on the surface of straw particles, Raman spectroscopy assessments were carried out at an ambient temperature in the Raman shift range of 800 – 1800 cm^{-1} using inVia Raman Microscope (Renishaw), equipped with a 785 nm wavelength laser beam.

2.3.3. X-ray diffraction

The X-ray diffraction (XRD) analysis was performed to examine the mineralogical composition of the wheat straw particles before and after pre-treatment and surface functionalisation processes by means of an Aeris Diffractometer (Bruker) with Cu-Kα radiation, 2θ of 5 – 90°, at 40 kV and 40 mA, and a wavelength of 1.542 Å. The crystallinity index (CI) was determined using an empirical technique provided by Segal et al. (1959) (Eq.1) based on the XRD data (Segal et al., 1959). The CI term is only valid for comparison purposes since it describes the order of crystallinity instead of the crystalline areas' crystallinity.

$$CI \quad (\%) = \frac{I_{002} - I_{amorph}}{I_{002}} \times 100 \tag{1}$$

Where: I_{002} is the maximum intensity of the (002) lattice diffraction and

Table 1
Mix formulations for PLA compressed strawboard manufacturing.

Mix formulation	Sample ID	PLA Compressed Strawboards		
		PLA matrices (vol%)	UN starw (vol%)	H+S starw (vol %)
Non-fuctionalisation samples	10UN	90	10	0
	20UN	80	20	0
	30UN	70	30	0
	40UN	60	40	0
	50UN	50	50	0
	10 H+S	90	0	10
	20 H+S	80	0	20
	30 H+S	70	0	30
	40 H+S	60	0	40
	50 H+S	50	0	50
0.1% Graphene surface fuctionalisation	10UN-G	90	10	0
	20UN-G	80	20	0
	30UN-G	70	30	0
	40UN-G	60	40	0
	50UN-G	50	50	0
	10 H+S-G	90	0	10
	20 H+S-G	80	0	20
	30 H+S-G	70	0	30
	40 H+S-G	60	0	40
	50 H+S-G	50	0	50
1% Attapulgite nano clay surface fuctionalisation	10UN-AT	90	10	0
	20UN-AT	80	20	0
	30UN-AT	70	30	0
	40UN-AT	60	40	0
	50UN-AT	50	50	0
	10 H+S-AT	90	0	10
	20 H+S-AT	80	0	20
	30 H+S-AT	70	0	30
	40 H+S-AT	60	0	40
	50 H+S-AT	50	0	50

* UN: untreated straw; H+S: Heat+Steam pre-treated straw; G: Graphene nanoplatelets; AT: Attapulgite nanoclay.

reflects both the crystalline and amorphous regions of the material (i.e., 2θ between 20° and 24°), and I_{amorph} implies the amorphous area (i.e., 2θ between 17° and 20°).

2.3.4. Thermogravimetric analysis

The effect of surface functionalisation on the thermal degradation of straw particles was investigated on 3 – 4 mg of straw samples using thermogravimetric analysis (TGA). TGA analysis was conducted via TA Instrument SDT Q600 under airflow with a heating range of 20–650 °C at a rate of 10 °C/min.

2.4. Mechanical properties

A total of 5 strawboard strips of size 100 mm x 20 mm x 20 mm were utilised to evaluate the tensile strength performance of each composition and mean values were taken as a representative. Tensile strength tests were performed employing an Instron 5969 universal testing machine equipped with wedge action tensile grips as per ASTM D3039/D3039 M.

2.5. Water absorption of bio-based composites strawboards

As per BS 5669 – 1:1989, the dimensional stability of bio-based composites, i.e., water absorption (WA), was measured on a batch of six samples of size 100 × 20 × 20 mm^3. The test was performed by submerging the samples in water at a constant temperature of 20 ± 2 °C. After 2 h and 24 h of exposure to the water, the weight of each sample was precisely measured using a digital scale with an accuracy of 0.01 (g). The water absorption percentages were determined as follows (Eq.2). A batch of three samples have been evaluated for each composition and the average results are reported.

$$WA(\%) = \left[\frac{W_2 - W_1}{W_1}\right] \times 100 \quad (2)$$

Where: WA is water absorption (%), W_1 (g) and W_2 (g) are the weights of samples before and after water immersion, respectively.

3. Result and discussion

3.1. Surface and microstructural changes due to pre-treatment and fuctionalisation

The microstructure of the wheat straw's cross-section before and after (H+S) pre-treatment were examined and using SEM. As shown in Fig. 4, H+S pre-treatment alternates the microstructure of wheat straw particles in terms of (i) parenchyma expansion and (ii) epidermis thickness reduction. Aforementioned desirable alternations lead to the deeper penetration of liquid PLA matrix inside the straw's parenchyma which in turn leads to an intimate bonding and subsequently, improving the strength of PLA compressed strawboard (Chougan et al., 2020; Ghaffar et al., 2017a). As presented in the author's previous work, an epidermis thickness reduction of about 47% occurred after (H+S) pre-treatment (Chougan et al., 2020). Reducing the size of the epidermal layer, which includes hydrophobic silicone and waxes, could be advantageous for improving interfacial interaction between polymer matrix and wheat straw owing to the lower hydrophobic contact area. Moreover, the results also indicated a 12% parenchyma expansion as a result of (H+S) pre-treatment, which guarantees a more in-depth penetration of the PLA matrix (see Fig. 4).

As seen in Figs. 5 and 6, SEM analysis was also performed on the surface of wheat straw before and after pre-treatment and surface functionalisation processes. The results indicated a continuous and smooth surface morphology for H+S straw particles (see Fig. 6 a and d), whereas UN samples showed a rough surface (see Fig. 5 a and d). The microstructure comparison of surface functionalised and non-functionalised straw particles confirm that AT and G particles have been effectively attached to the straw's surface. However, due to the lower hydrophobic contact area of the H+S samples, a higher quantity of AT and G particles were presented on the pre-treated samples. In order to prove the aforementioned statements, FTIR-ATR spectroscopy (Fig. 7) was used to characterise the surface chemical distribution of pre-treated and untreated straw. The bands at 1595 cm^{-1} and 1510 cm^{-1} represent the aromatic ring stretch of lignin (Yang et al., 2020). As shown in (Fig. 7-i), the lignin peaks for pre-treated straw samples was slightly attenuated than that of untreated straw samples, which implies a partial lignin extraction as a result of H+S pre-treatment. The major components of extractives and hemicellulose are represented by mode at 1735 cm^{-1}, which encompasses carboxyl groups in the acids and esters of acetic, p-coumeric, ferulic, and uronic acids (Alemdar and Sain, 2008a). As seen in Fig. 7-ii, comparing to UN straw, the intensity of this band was mitigated in the H+S samples. Peaks at bands 2920 cm^{-1} and 2850 cm^{-1} show asymmetric and symmetric CH_2 stretching bands that correspond to the aliphatic fractions of waxes (Saari et al., 2014). The results confirmed that H+S straw samples contain lower frictions of wax and inorganic compounds than that of UN samples (see Fig. 7-iii). This suggests that pre-treatment reduces the waxes and inorganic chemicals on the surface of straw particles.

As evident in Fig. 5 (b and e) and Fig. 6 (b and e), for both pre-treated

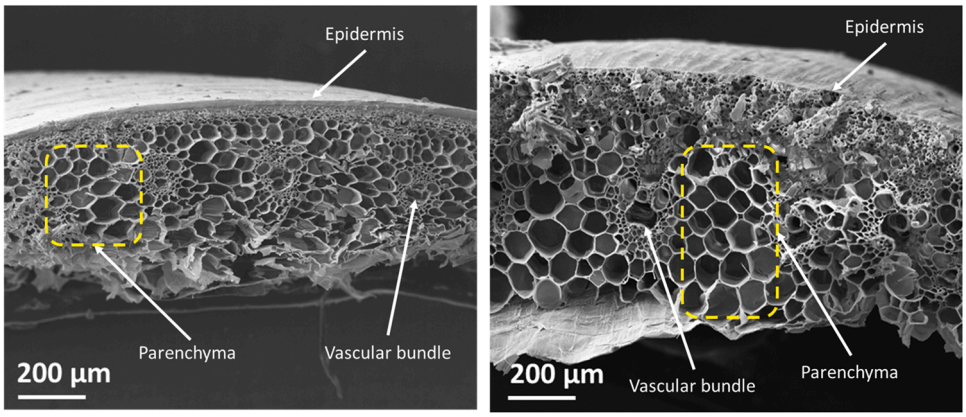

Fig. 4. SEM images of internode cross-section profile of (a) untreated (UN) and (b) pre-treated (H+S) straw particles.

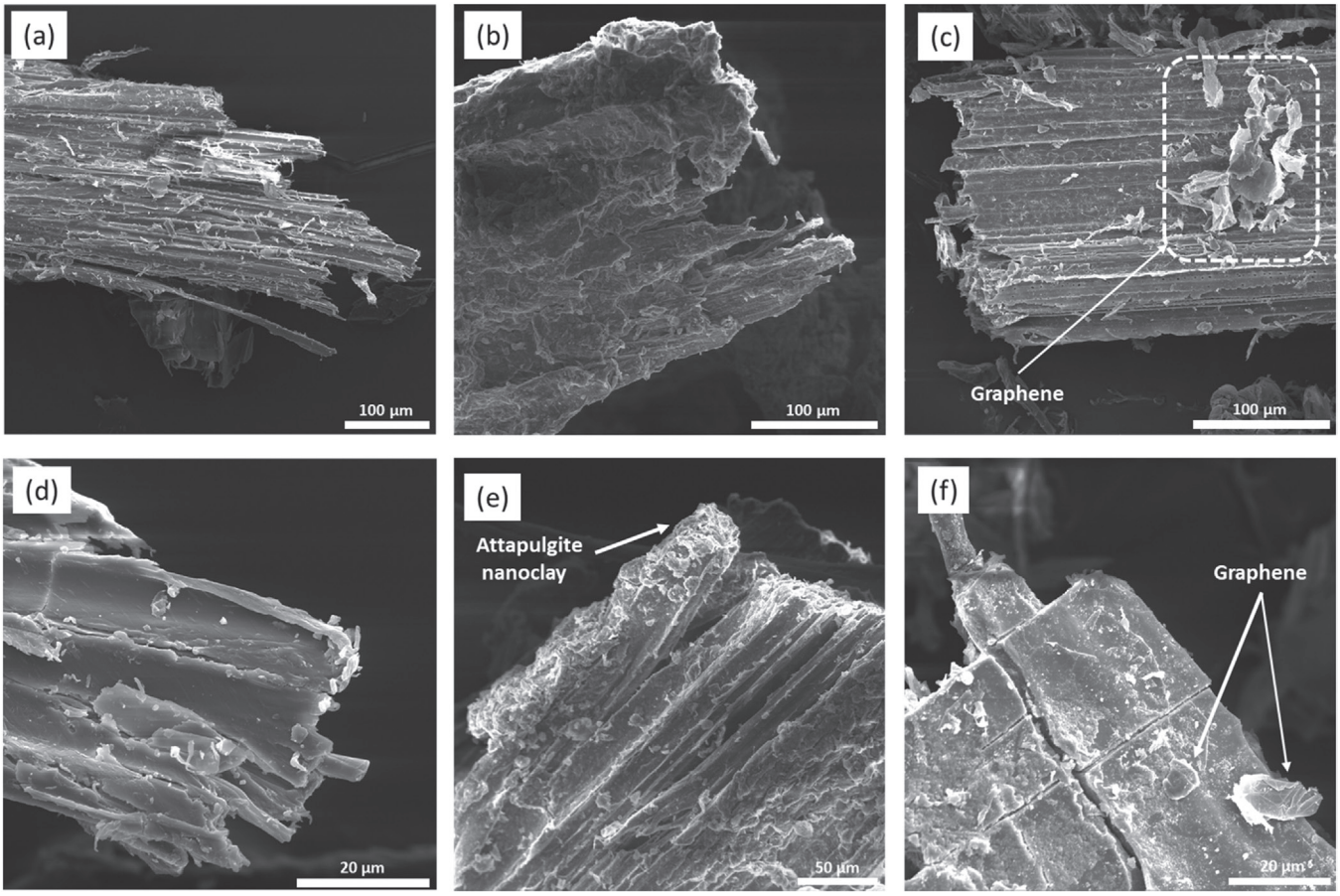

Fig. 5. SEM images of (a and d) untreated (UN) straw particles and their composites with (b and e) AT nanoclays and (c and f) graphene nanoplatelets.

and untreated samples, the distinctive attapulgite nanoclay particles are effectively covering the straw surface. Fig. 5 (c and f) and Fig. 6 (c and f), on the other hand, demonstrate isolated graphene nanoplatelets sticking to the straw surface. In order to validate the surface functionalisation, Raman spectroscopy test was performed (see Fig. 8**)** as an intuitive method to investigate the presence of functionalising agents on the surface of straw particles. Two typical characteristic peaks of graphene particles, i.e., D band at 1335 cm^{-1}, attributable to the carbon lattice disorder specific of edges and defects in the aromatic structure, and G band at 1585 cm^{-1}, referring to the C sp2 in-plane vibration of the graphene lattice, were clearly observed on the straw particles' surface (Owens, 2015). As evident in Fig. 8, UN-G and H+S-G straw samples both have typical characteristic peaks of graphene particles. Typical characteristic signals of attapulgite nanoclay particles were also detected. For UN-AT and H+S-AT samples, the distinctive peaks of AT were observed. None of the aforementioned characteristic peaks can be ascertained on neat, i.e., not functionalised, UN and H+S straws (marked in blue and green, respectively), indicating that AT and G particles homogeneously covered the straw particles.

3.2. *Thermogravimetric analysis*

Thermogravimetric analysis (TGA) was conducted on wheat straw particles before and after surface functionalisation to validate their

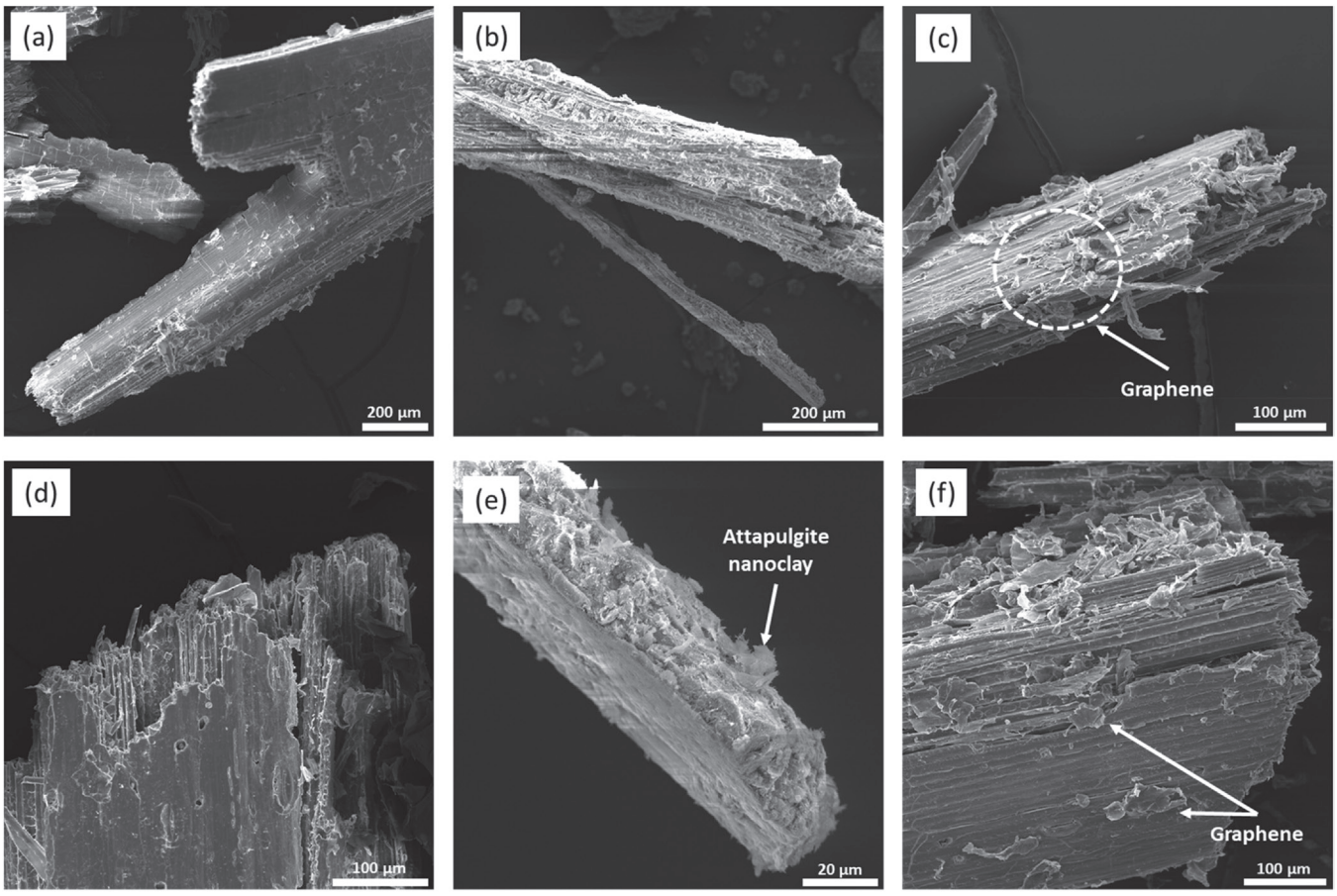

Fig. 6. SEM images of (a and d) pre-treated (H+S) straw particles and their composites with (b and e) AT nanoclays and (c and f) graphene nanoplatelets.

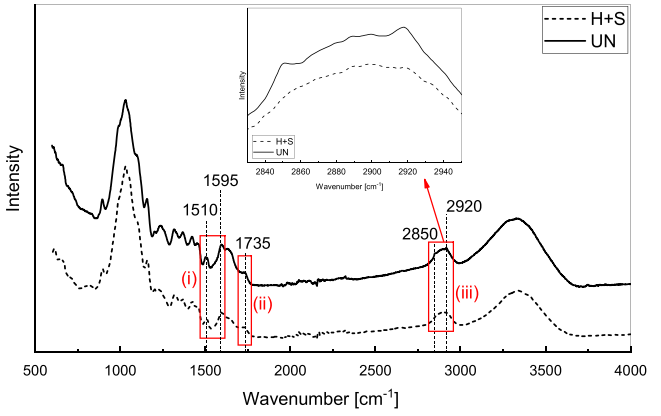

Fig. 7. FTIR-ATR spectrum of untreated (UN) and pre-treated (H+S) straw particles.

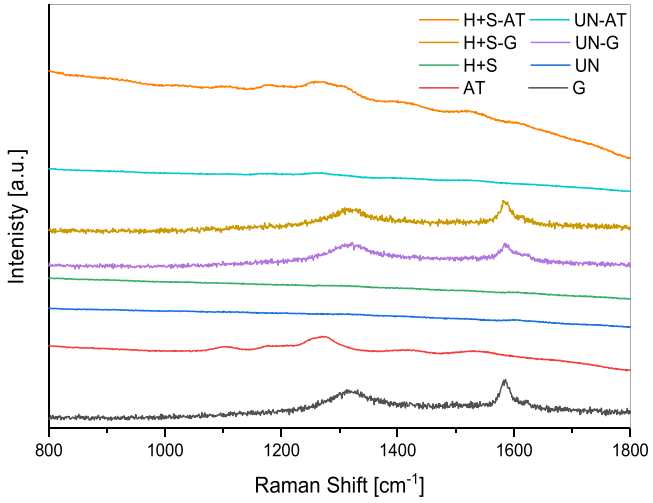

Fig. 8. Raman spectra of untreated, and pre-treated straw particles and their composites with G and AT nanoparticles.

thermal stability, as shown in Fig. 9. TGA analysis presented in the thermograms, which revealed three distinct stages of thermal degradation. The initial stage of the straw sample's weight loss was observed at 100–150 °C owing to the moisture evaporation. The cellulose and hemicellulose in the straw sample broke down at temperature range between 250 and 350 °C, resulting in substantial weight loss. The decomposition of non-cellulosic components, particularly in the case of graphene nanoplatelets, caused the ultimate weight loss in the temperature range of 500–600 °C. However, the aforementioned temperature range (i.e., 500–600 °C) is insufficient to degrade AT nanoclay particles (Ergudenler and Ghaly, 1992; Ghaffar and Fan, 2015). Several authors (Ghaffar and Fan, 2015; Zandi et al., 2019) suggested a direct correlation between the onset of degradation temperature and the thermal stability of straw, more specifically, higher onset of degradationindicates enhanced thermal stability of straw. As it can be seen in Fig. 9-**i**, due to the extraction of waxy compounds and hemicelluloses induced by the H+S pre-treatment, the onset of degradation temperature for H+S pre-treated straw and its corresponded surface functionalised particles (i.e., 255 °C for H+S, 254 °C for H+S-G, and 276 °C for

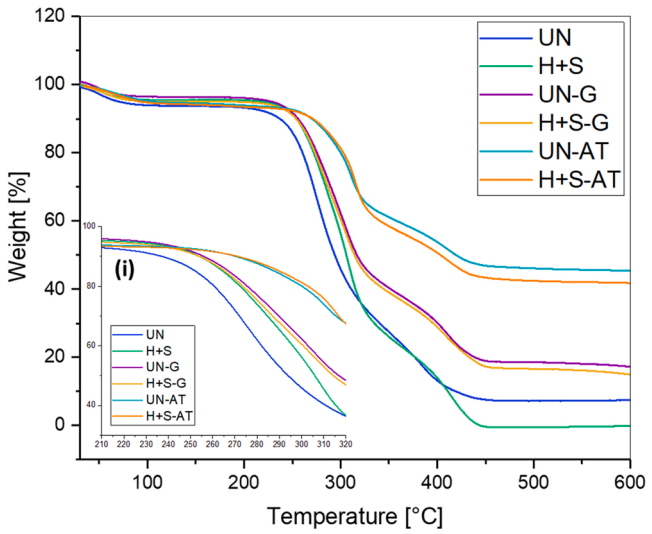

Fig. 9. TGA thermogram data of untreated and H+S pre-treated wheat straw particles with and without surface functionalisation.

H+S-AT) are relatively higher than that of untreated straw samples (i.e., 248 °C for UN, 253 °C for UN-G, 265 °C for UN-AT).

The high content of silica and ash silica on the surface of straw particles makes it challenging to incorporate these components into bio-based composites applications. According to Qin et al. (2011), the residual weight at 600 °C corresponds to the remaining ash content (Qin et al., 2011). Compared to the UN samples, the ash content of H+S samples is substantially lower. The reduction in the ash and silica content of the straw particles enhances the interfacial interaction between the straw and PLA matrix, therefore, improving the performance of PLA compressed strawboards.

3.3. Pre-treatment and surface functionalisation effect on crystallinity index

Fig. 10 exhibits XRD patterns of G, AT, and functionalised straw particles to analyse the crystalline phases of specimens. All of them are typical for cellulosic materials. The maximum intensity was recorded at $2\theta = 21.55° - 22°$, corresponding to the 002 lattices (Ghaffar and Fan, 2015; Kaushik et al., 2010). Furthermore, the existence of cellulose in the form of cellulose I crystal was confirmed by the secondary peak

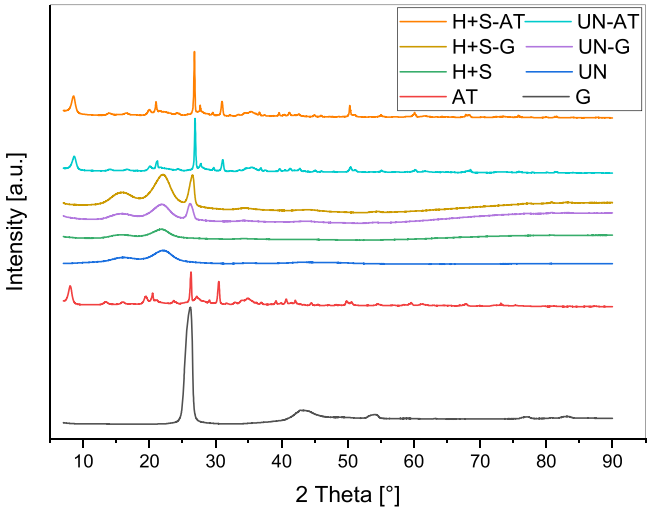

Fig. 10. X-ray diffraction patterns of untreated and H+S pre-treated wheat straw with and without surface functionalisations.

around $2\theta = 18°$. The crystallinity index of all straw samples is shown in Table 2. The crystallinity index of UN straw particles was calculated to be 55.6%. The crystallinity index increased by approximately 3% following H+S pre-treatment and reached 57.4%. The extraction of fundamentally amorphous polymers within the constituents of wheat straw, particularly lignin and hemicellulose, is directly proportional to the mere increase in crystallinity index induced by the H+S pre-treatment (Alemdar and Sain, 2008b). According to Zhu et al. (2006), the rise in cellulose content is related to the solubilisation of its constituents (Zhu et al., 2006). The increase in the content of crystalline cellulose in the straw particles leads to enhanced thermal stability and strength of the individual biomass particles (Chen et al., 2021).

The findings suggest that both straw samples functionalised with graphene particles, i.e., H+S-G and UN-G, have distinct XRD patterns compared to their correspondent H+S and UN straw samples. The basal reflection peak (002) of graphene flakes at $2 = 26.2°$ is visible on the straw particles surface after the functionalisation process (Lu and Ouyang, 2017; Lv et al., 2013). Moreover, (110), (200), (040), (231) and (161) crystallographic planes of attapulgite particles were detected in both H+S-AT and UN-AT samples at $2\theta = 8.05°$, 13.29°, 19.5°, 26.7°, and 31.02°, respectively (Tong et al., 2021). The above findings indicate that straw samples were effectively functionalised by G and AT nano-particles. The results of crystallinity indices also indicated that the functionalisation of straw with AT and G induced a positive effect in terms of increasing the crystallinity index (CI). In Table 2, the CI values increased as the surface functionalisation was applied. However, the most eminent CI improvement was registered for pre-treated straw samples. When compared to the counterpart sample without surface functionalisation (i.e., H+S sample), the CI was enhanced by 2% and 10% for (H+S-G) and (H+S-AT), respectively. This improved the tensile strength of the individual biomass particles and consequently enhanced the resilience of bio-based composites (Ghaffar et al., 2017a).

3.4. Tensile performance improvements of PLA compressed strawboards

As shown in Fig. 11, an investigation of straw board's tensile strength was conducted to evaluate the influence of pre-treatment and surface functionalisation processes.

In general, the tensile strength of bio-based composites is highly reliant on the strength of individual straw particles, straw quantity, and the quality of the interfacial bond between the straw particle and PLA matrix (Ghaffar et al., 2017a; Pereira et al., 2013). In all compositions, it is evident that the tensile strength of bio-based composites displayed a descending trend with the rise of straw content from 10 vol% to 50 vol %. However, the results indicated that the introduction of H+S pre-treatment appeared to have a better impact on the tensile strength exhibited by the samples. The inclusion of 10, 20, 30, 40, and 50 vol% pre-treated straw particles (i.e., H+S) enhanced the tensile strength by 46%, 69%, 127%, 66%, and 345%, respectively, compared to their corresponding bio-based composites made of (UN) straw particles. The remarkable improvement in the tensile performance of (H+S) bio-based composites compared to (UN) counterparts could be associated with (i) improvements in straw's wetting properties leading to enhanced interfacial bonding between PLA matrix and straw particles (Rakesh Kumar,

Table 2
Crystallinity index comparison of untreated and H+S pre-treated wheat straw particles with and without surface functionalisation.

Sample ID	Crystallinity index [%]
UN	55.6
UN-G	58.1
UN-AT	55.7
H+S	57.4
H+S-G	58.4
H+S-AT	63.0

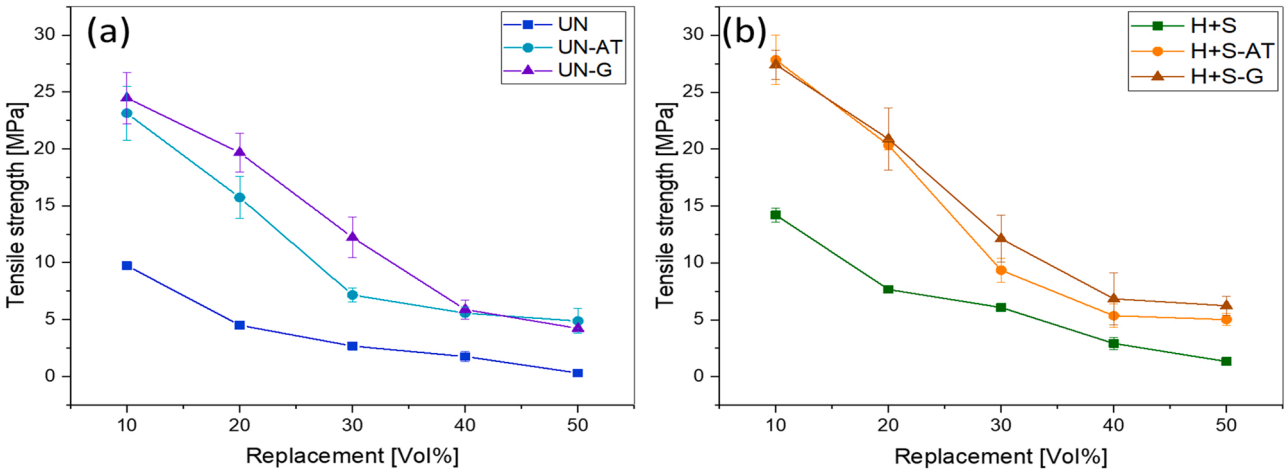

Fig. 11. Tensile strength of bio-based composites with different percentage of untreated (UN) and pre-treated (H+S) straw particles and their composites with G and AT nanoparticles.

Sangeeta Obrai, 2011), (ii) the cell walls expansion caused by the steaming stage (S) allowing more PLA polymer in the liquid state to penetrate within the enlarged straw cells and thereby increasing mechanical entanglement, (iii) higher crystallinity index of (H+S) straw samples, indicating that their strength has improved due to the existence of more stable cellulose chains in their structure. Besides the aforementioned improvements in straw's surface functioning and PLA-straw interface, Ghaffar et al. (2017) reported that the tensile strength of (H+S) individual strands reached 88.9 MPa, which is 35% higher than that of (UN) strands (i.e., 66 MPa) (Ghaffar et al., 2017a). The tensile strength of the surface functionalised composite samples was also shown to follow a similar trend. In all straw contents, H+S functionalized samples (i.e., H+S-AT and H+S-G) exhibited higher or comparable overall tensile strength than UN functionalised samples (i.e., UN-AT and UN-G). Moreover, the results also highlight the superior impact of AT and G surface functionalisation techniques on the tensile strength of (UN) and (H+S) bio-based composites. The most significant enhancement in tensile strength was registered in the samples with the highest percentage (i.e., 50 vol%) of surface functionalised straw particles. The results indicated that the AT and G surface functionalisation processes increased the tensile strength from 0.3 MPa for the (50UN) sample to 4.9 MPa and 4.3 MPa for (50UN-AT) and (50UN-G), respectively. In the case of H+S pre-treated samples, remarkable improvements of approximately 276% and 367% were registered for (50 H+S-AT) and (50 H+S-G), respectively, when compared to that of (50 H+S) samples. The same incremental trend in tensile strength was reported by Scaffaro et al. (2020) and Zhu et al. (2019) (Scaffaro et al., 2020; Zhu et al., 2019). As reported in previous research, surface functionalisation processes have been considered to provide a crosslinking effect to enhance the interfacial bonding between straw and PLA matrix (Scaffaro et al.,

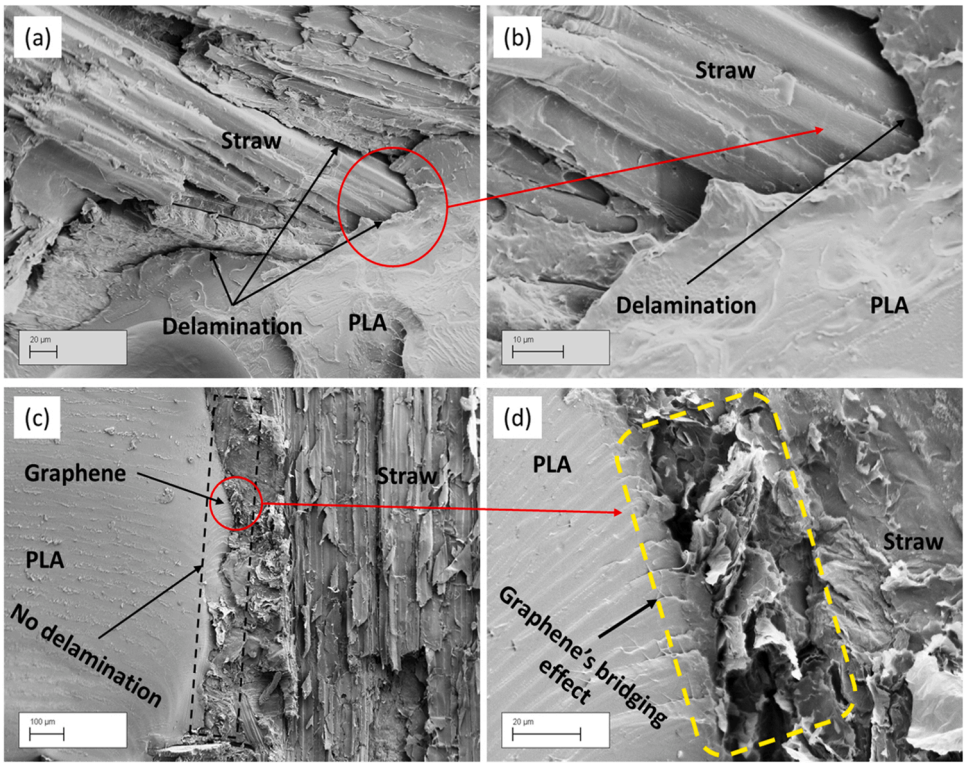

Fig. 12. SEM images of (a and b) H+S samples and (c and d) H+S-G.

2020; Zhu et al., 2019). Both surface functionalising agents, i.e., graphene and attapulgite, were dispensed to improve the tensile performance of functionalised strawboards. As shown in Fig. 12, graphene particles on the surface of pre-treated straw effectively bridge the gap between functionalised straw particles and PLA matrix, resulting in an intimate interfacial connection. It is evident that the delamination phenomenon is significantly decreased as a result of G surface functionalisation. The effect is critical since the inclusion of a small quantity of AT and G is capable of overcoming the tensile strength loss that occurs when straw particles are added, which is the most prevalent drawback of bio-based composites. The developed strawboard in this study considered as a high-performance bio-based composite. The performance of the strawboard is related to production method, and the matrix used and its compatibility with wheat straw. The most widely used matrices in manufacturing processes are urea-formaldehyde (UF) and phenol-formaldehyde (PF). However, UF offers low bonding properties between straw particles due to the hydrophobic nature of straw. It is reported that strawboards bonded with UF have 6.3 MPa tensile strength on average (Wool and Sun, 2011). Mo et al. (2001) has also been reported that strawboards manufactured with soy protein isolate and methylene diphenyl diisocyanate adhesives provide the maximum tensile strength of 0.27 MPa and 0.49 MPa, respectively (Mo et al., 2003). Although several studies achieved better tensile strength than this study, their preparation and manufacturing procedures (i.e., compounding and injection moulding) are energy-consuming and are not feasible for producing straw boards on a large scale. A study conducted by Fan et al. (2018) investigated the performance of PLA bio-based composites reinforced by wheat straw, which was treated with polydopamine. Their results indicated that the tensile strength of PLA bio-based composites increased from 3.54 MPa for the samples containing untreated wheat straw to 6.75 MPa for the samples containing polydopamine treated wheat straw (Fan et al., 2018). The outcomes of present study indicate that the utilised pre-treatment coupled with nano functionalisation techniques contributes to manufacturing strawboards with high-performance characteristics.

3.5. Water absorption of functionalised PLA compressed strawboards

According to acquired test results, compressed strawboards comprising 10 vol.-% and 20 vol.-% straw particles and their functionalised derivatives performed the best in terms of tensile strength. Therefore, they were selected to be assessed as appropriate compositions for physical property characterisation. Water absorption (WA) test was adopted to determine the stability of PLA compressed strawboards after 2 and 24 h of immersing in water. In general, the water absorption rate of bio-based composite depends on several factors such as type of matrix and reinforcing biomass, temperature, humidity, and biomass content. It can be seen in Fig. 13 that the inclusion of a higher straw particle content leads to increased water absorption percentages which are in agreement with a previous study (Dhakal et al., 2007). The water absorption of all bio-based composites increased over testing time. After 2 h of immersion, the results showed that water intake increased from 1.6% and 2.3% for 10UN and 20UN, respectively, to 1.8% and 3% for 10 H+S and 20 H+S, respectively. A similar trend was also observed for samples after 24 h of immersion in water. The same effect was also observed for all the compressed strawboards with surface functionalised straw particles. It can be concluded that the H+S pre-treatment of straw particles led to an increased water absorption of the PLA compressed strawboard. This observation could be due to a reduction in the hydrophobicity of straw particles after the pre-treatment as evidenced by reduced wax and silica concentration recorded from the surface chemical functional group analysis as shown in Fig. 7. Additionally, increased surface porosity of straw particles caused by partial hemicellulose and lignin degradation, could enable easier penetration of water molecules to the compressed strawboards, as previously reported by Zeng et al. (2018) (Zheng et al., 2018). The surface functionalisation technique using both graphene nanoplatelets and attapulgite nanoclay was found to be effective in decreasing strawboards water penetration. However, it has been found that samples fabricated with graphene surface functionalised straws are more efficient and have slightly lower water absorption than their counterparts manufactured with attapulgite nanoclay. The results indicated that after 24 h of immersion, the water absorptions of 10UN-G, 20UN-G, 10 H+S-G, and 20 H+S-G are 10%, 8%, 20%, and 19% lower than the values registered for 10UN, 20UN, 10 H+S, and 20 H+S samples, respectively. The aforementioned results could be associated with the better compatibility of surface functionalised straws with PLA matrix, which leads to a stronger straw-matrix bonding and denser structure within the strawboards.

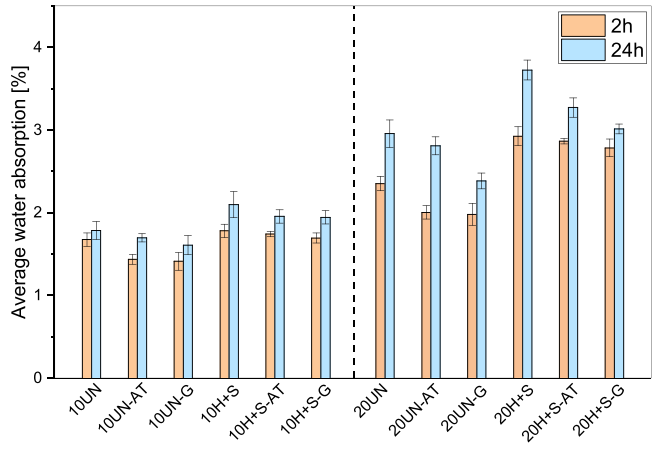

Fig. 13. Water absorption of bio-composites after 2 h and 24 h of water exposure.

4. Conclusion

The main objective of this research was to investigate the impact of pre-treated and surface functionalised straw particles as reinforcing agents in PLA compressed strawboards. Two nano functional materials (i.e., graphene nanoplatelets and attapulgite nanoclay) were employed to provide a cross-linking effect between straw particles and the PLA matrix. Significant alterations were observed on wheat straw particles via characterisation tests as a result of pre-treatment and surface functionalisation processes. All the bio-based composites employing graphene nanoplatelets as a surface functionalising agent were shown to be the best performing composites in terms of tensile property. The 10 H+S-AT and 10 H+S-G samples exhibited maximum tensile strengths of 28 MPa and 27 MPa, respectively, which are significantly higher than the 9.7 MPa recorded for the 10UN sample. Water absorption percentages of 1.6%, and 1.9% were registered for 10UN-G and 10 H+S-G, respectively after 24 h of submersion in water. Employing the minimum amount of graphene nanoplatelets and attapulgite nanoclay as an emerging surface functionalising (or crosslinking) agent in PLA compressed strawboards proved to be suitable for boosting straw incorporation in PLA based composites. Surface functionalised wheat straw particles developed in this study exhibit a promising breakthrough that can be used as a benchmark in producing high-performance bio-based composites.

CRediT authorship contribution statement

Mehdi Chougan: Conceptualization, Methodology, Validation, Investigation, Writing – original draft, Visualization. **Seyed Hamidreza Ghaffar**: Conceptualization, Methodology, Validation, Investigation, Resources, Writing – original draft, Visualization, Supervision, Funding acquisition. **Ewa Mijowska**: Methodology, Validation, Investigation, Writing – review & editing. **Wojciech Kukułka**: Methodology,

Validation, Investigation, Writing – review & editing. **Pawel Sikora**: Methodology, Validation, Investigation, Writing – review & editing.

Declaration of Competing Interest

The authors declare that they have no known competing financial interests or personal relationships that could have appeared to influence the work reported in this paper.

Acknowledgement

This work was funded as part of the HP-CSB project, which has received funding from the Engineering and Physical Sciences Research Council with the following reference: EP/S026487/1. The authors acknowledge Nanesa S.r.l for graphene material supply.

References

Alemdar, A., Sain, M., 2008a. Isolation and characterization of nanofibers from agricultural residues - Wheat straw and soy hulls. Bioresour. Technol. 99, 1664–1671. https://doi.org/10.1016/j.biortech.2007.04.029.

Alemdar, A., Sain, M., 2008b. Biocomposites from wheat straw nanofibers: Morphology, thermal and mechanical properties. Compos. Sci. Technol. 68, 557–565. https://doi.org/10.1016/j.compscitech.2007.05.044.

Chen, K., Li, P., Li, Xingong, Liao, C., Li, Xianjun, Zuo, Y., 2021. Effect of silane coupling agent on compatibility interface and properties of wheat straw/polylactic acid composites. Int. J. Biol. Macromol. 182, 2108–2116. https://doi.org/10.1016/j.ijbiomac.2021.05.207.

Chougan, M., Ghaffar, S.H., Al-Kheetan, M.J., Gecevicius, M., 2020. Wheat straw pre-treatments using eco-friendly strategies for enhancing the tensile properties of bio-based polylactic acid composites. Ind. Crops Prod. 155 https://doi.org/10.1016/j.indcrop.2020.112836.

Chougan, M., Ghaffar, S.H., Sikora, P., Chung, S.Y., Rucinska, T., Stephan, D., Albar, A., Swash, M.R., 2021. Investigation of additive incorporation on rheological, microstructural and mechanical properties of 3D printable alkali-activated materials. Mater. Des. 202, 109574 https://doi.org/10.1016/j.matdes.2021.109574.

Chougan, M., Ghaffar, S.H., Sikora, P., Mijowska, E., Kukułka, W., Stephan, D., 2022. Boosting Portland cement-free composite performance via alkali-activation and reinforcement with pre-treated functionalised wheat straw. Ind. Crops Prod. 178 https://doi.org/10.1016/j.indcrop.2022.114648.

Das, P.P., Chaudhary, V., Ahmad, F., Manral, A., Gupta, S., Gupta, P., 2022. Acoustic performance of natural fiber reinforced polymer composites: Influencing factors, future scope, challenges, and applications. Polym. Compos. 43, 1221–1237. https://doi.org/10.1002/pc.26455.

Dhakal, H.N., Zhang, Z.Y., Richardson, M.O.W., 2007. Effect of water absorption on the mechanical properties of hemp fibre reinforced unsaturated polyester composites. Compos. Sci. Technol. 67, 1674–1683. https://doi.org/10.1016/j.compscitech.2006.06.019.

Ergudenler, A., Ghaly, A., 1992. Determination of reaction kinetics of wheat straw using thermogravimetric analysis. Appl. Biochem. Biotechnol. 34 https://doi.org/10.1007/BF02920535.

Fan, Q., Han, G., Cheng, W., Tian, H., Wang, D., Xuan, L., 2018. Effect of intercalation structure of organo-modified montmorillonite/polylactic acid on wheat straw fiber/polylactic acid composites. Polymers (Basel) 10, 1–14. https://doi.org/10.3390/polym10080896.

Ghaffar, S.H., Fan, M., 2017. An aggregated understanding of physicochemical properties and surface functionalities of wheat straw node and internode. Ind. Crops Prod. 95, 207–215. https://doi.org/10.1016/j.indcrop.2016.10.045.

Ghaffar, S.H., Fan, M., 2015. Differential behaviour of nodes and internodes of wheat straw with various pre-treatments. Biomass and Bioenergy 83, 373–382. https://doi.org/10.1016/j.biombioe.2015.10.020.

Ghaffar, S.H., Fan, M., McVicar, B., 2017a. Interfacial properties with bonding and failure mechanisms of wheat straw node and internode. Compos. Part A Appl. Sci. Manuf. 99, 102–112. https://doi.org/10.1016/j.compositesa.2017.04.005.

Ghaffar, S.H., Fan, M., Zhou, Y., Abo Madyan, O., 2017b. Detailed Analysis of Wheat Straw Node and Internode for Their Prospective Efficient Utilization. J. Agric. Food Chem. 65, 9069–9077. https://doi.org/10.1021/acs.jafc.7b03304.

Gupta, B., Revagade, N., Hilborn, J., 2007. Poly(lactic acid) fiber: An overview. Prog. Polym. Sci. 32, 455–482. https://doi.org/10.1016/j.progpolymsci.2007.01.005.

Hýsková, P., Hýsek, Š., Schönfelder, O., Šedivka, P., Lexa, M., Jarský, V., 2020. Utilization of agricultural rests: Straw-based composite panels made from enzymatic modified wheat and rapeseed straw. Ind. Crops Prod. 144 https://doi.org/10.1016/j.indcrop.2019.112067.

Kaushik, A., Singh, M., Verma, G., 2010. Green nanocomposites based on thermoplastic starch and steam exploded cellulose nanofibrils from wheat straw. Carbohydr. Polym. 82, 337–345. https://doi.org/10.1016/j.carbpol.2010.04.063.

Laadila, M.A., Hegde, K., Rouissi, T., Brar, S.K., Galvez, R., Sorelli, L., Cheikh, R., Ben, Paiva, M., Abokitse, K., 2017. Green synthesis of novel biocomposites from treated cellulosic fibers and recycled bio-plastic polylactic acid. J. Clean. Prod. 164, 575–586. https://doi.org/10.1016/j.jclepro.2017.06.235.

Lamastra, F.R., Chougan, M., Marotta, E., Ciattini, S., Ghaffar, S.H., Caporali, S., Vivio, F., Montesperelli, G., Ianniruberto, U., Al-Kheetan, M.J., Bianco, A., 2021. Toward a better understanding of multifunctional cement-based materials: The impact of graphite nanoplatelets (GNPs). Ceram. Int. 47, 20019–20031. https://doi.org/10.1016/j.ceramint.2021.04.012.

Liu, M., Thygesen, A., Summerscales, J., Meyer, A.S., 2017. Targeted pre-treatment of hemp bast fibres for optimal performance in biocomposite materials: A review. Ind. Crops Prod. 108, 660–683. https://doi.org/10.1016/j.indcrop.2017.07.027.

Lu, L., Ouyang, D., 2017. Properties of Cement Mortar and Ultra-High Strength Concrete Incorporating Graphene Oxide Nanosheets. Nanomaterials 7, 187. https://doi.org/10.3390/nano7070187.

Lv, S., Ma, Y., Qiu, C., Zhou, Q., 2013. Regulation of GO on cement hydration crystals and its toughening effect. Mag. Concr. Res. 65, 1246–1254. https://doi.org/10.1680/macr.13.00190.

Melo, R.R., Stangerlin, D.M., Santana, R.R.C., Pedrosa, T.D., 2014. Physical and mechanical properties of particleboard manufactured from wood, bamboo and rice husk. Mater. Res. 17, 682–686. https://doi.org/10.1590/S1516-14392014005000052.

Mo, X., Cheng, E., Wang, D., Sun, X.S., 2003. Physical properties of medium-density wheat straw particleboard using different adhesives. Ind. Crops Prod. 18, 47–53. https://doi.org/10.1016/S0926-6690(03)00032-3.

Mousa, N., Galiwango, E., Haris, S., Al-marzouqi, A.H., Abu-jdayil, B., Caires, Y.L., 2022. A new green composite based on plasticized polylactic acid mixed with date palm waste for single-use plastics applications. Polymers (Basel) 14. https://doi.org/10.3390/polym14030574.

Owens, F.J., 2015. Raman and surface-enhanced Raman spectroscopy evidence for oxidation-induced decomposition of graphite. Mol. Phys. 113, 1280–1283. https://doi.org/10.1080/00268976.2014.986237.

Pawar, K.S., Bagha, A.K., Bahl, S., Nandan, D., 2022, Significant Applications of Composite and Natural Materials for Vibration and Noise Control: A Review, in: Advancement in Materials, Manufacturing and Energy Engineering. ⟨https://doi.org/10.1007/978–981-16–8341-1_17⟩.

Pereira, C.L., Savastano, H., Payá, J., Santos, S.F., Borrachero, M.V., Monzó, J., Soriano, L., 2013. Use of highly reactive rice husk ash in the production of cement matrix reinforced with green coconut fiber. Ind. Crops Prod. 49, 88–96. https://doi.org/10.1016/j.indcrop.2013.04.038.

Prakash, S.O., Sahu, P., Madhan, M., Johnson Santhosh, A., 2022. A review on natural fibre-reinforced biopolymer composites: properties and applications. Int. J. Polym. Sci. 2022. https://doi.org/10.1155/2022/7820731.

Qin, L., Qiu, J., Liu, M., Ding, S., Shao, L., Lü, S., Zhang, G., Zhao, Y., Fu, X., 2011. Mechanical and thermal properties of poly(lactic acid) composites with rice straw fiber modified by poly(butyl acrylate). Chem. Eng. J. 166, 772–778. https://doi.org/10.1016/j.cej.2010.11.039.

Rakesh Kumar, Sangeeta Obrai, A.S., 2011. Chemical modifications of natural fiber for composite material. Der Chem. Sin. 4, 219–228.

Saari, N., Hashim, R., Sulaiman, O., Hiziroglu, S., Sato, M., Sugimoto, T., 2014. Properties of steam treated binderless particleboard made from oil palm trunks. . Compos. Part B Eng. 56, 344–349. https://doi.org/10.1016/j.compositesb.2013.08.062.

Scaffaro, R., Maio, A., Gulino, E.F., Pitarresi, G., 2020. Lignocellulosic fillers and graphene nanoplatelets as hybrid reinforcement for polylactic acid: Effect on mechanical properties and degradability. Compos. Sci. Technol. 190, 108008 https://doi.org/10.1016/j.compscitech.2020.108008.

Segal, L., Creely, J.J., Martin, A.E., Conrad, C.M., 1959. An empirical method for estimating the degree of crystallinity of native cellulose using the X-ray diffractometer. Text. Res. J. 29, 786–794. https://doi.org/10.1177/004051755902901003.

Tawakkal, I.S.M.A., Cran, M.J., Miltz, J., Bigger, S.W., 2014. A review of poly(lactic acid)-based materials for antimicrobial packaging. J. Food Sci. 79 https://doi.org/10.1111/1750-3841.12534.

Tong, H., Liu, X., Liu, Y., Zhang, H., Li, X., 2021. Polyaniline modified attapulgite incorporated in alkyd paint for carbon steel corrosion inhibition. Corros. Eng. Sci. Technol. 0, 1–8. https://doi.org/10.1080/1478422x.2021.1931646.

Tribot, A., Delattre, C., Badel, E., Dussap, C.G., Michaud, P., de Baynast, H., 2018. Design of experiments for bio-based composites with lignosulfonates matrix and corn cob fibers. Ind. Crops Prod. 123, 539–545. https://doi.org/10.1016/j.indcrop.2018.07.019.

Wool, R., Sun, X., 2011. Bio-Based Polymers and Composites. Elsevier Science.

Yang, Y., Shen, H., Qiu, J., 2020. Bio-inspired self-bonding nanofibrillated cellulose composite: A response surface methodology for optimization of processing variables in binderless biomass materials produced from wheat-straw-lignocelluloses. Ind. Crops Prod. 149, 112335 https://doi.org/10.1016/j.indcrop.2020.112335.

Zandi, A., Zanganeh, A., Hemmati, F., Mohammadi-Roshandeh, J., 2019. Thermal and biodegradation properties of poly(lactic acid)/rice straw composites: effects of modified pulping products. Iran. Polym. J. (English Ed. 28, 403–415. https://doi.org/10.1007/s13726-019-00709-3.

Zheng, Q., Zhou, T., Wang, Y., Cao, X., Wu, S., Zhao, M., Wang, H., Xu, M., Zheng, B., Zheng, J., Guan, X., 2018. Pretreatment of wheat straw leads to structural changes and improved enzymatic hydrolysis. Sci. Rep. 8, 1–9. https://doi.org/10.1038/s41598-018-19517-5.

Zhu, L., Qiu, J., Liu, W., Sakai, E., 2019. Mechanical and thermal properties of rice Straw / PLA modi fi ed by nano Attapulgite / PLA interfacial layer. In: Compos. Commun., 13, pp. 18–21. https://doi.org/10.1016/j.coco.2019.02.001.

Zhu, S., Wu, Y., Yu, Z., Wang, C., Yu, F., Jin, S., Ding, Y., Chi, R., Liao, J., Zhang, Y., 2006. Comparison of three microwave/chemical pretreatment processes for

enzymatic hydrolysis of rice straw. Biosyst. Eng. 93, 279–283. https://doi.org/10.1016/j.biosystemseng.2005.11.013.